Molecular Therapy
Nucleic Acids
Original Article

DRAM1 increases the secretion of PKM2-enriched EVs from hepatocytes to promote macrophage activation and disease progression in ALD

Jie Tan,[1,4] Jie Zhang,[1,4] Mengke Wang,[1] Yifen Wang,[1] Mengzhen Dong,[1] Xuefeng Ma,[1] Baokai Sun,[1] Shousheng Liu,[2] Zhenzhen Zhao,[2] Lizhen Chen,[1] Wenwen Jin,[1] Kai Liu,[3] Yongning Xin,[1] and Likun Zhuang[2]

[1]Department of Infectious Diseases, Qingdao Municipal Hospital, Qingdao University, Qingdao 266011, China; [2]Clinical Research Center, Qingdao Municipal Hospital, Qingdao University, Qingdao 266071, China; [3]Beijing Institute of Hepatology, Beijing Youan Hospital, Capital Medical University, Beijing 100069, China

DNA damage-regulated autophagy modulator 1 (DRAM1) could play important roles in inflammation and hepatic apoptosis, while its roles in alcohol-related liver disease (ALD), which is characterized by hepatic inflammation and apoptosis, are still unclear. In this study, we explored the expression, role, and mechanism of DRAM1 in ALD. Firstly, our results showed that DRAM1 was significantly increased in liver tissues of mice at the early stage of alcohol treatment. In addition, DRAM1 knockout reduced, and liver-specific overexpression of DRAM1 aggravated, alcohol-induced hepatic steatosis, injury, and expressions of M1 macrophage markers in mice. Furthermore, ethanol-induced DRAM1 of hepatic cells increased pyruvate kinase M2 (PKM2)-enriched extracellular vesicles (EVs), and ectosomes derived from hepatic cells with DRAM1 overexpression promoted macrophage activation. Mechanistic investigations showed that DRAM1 interacted with PKM2 and increased the PKM2 level in plasma membrane. At last, DRAM1 was significantly increased in liver tissues of ALD patients, and it was positively correlated with M1 macrophage markers. Taken together, this study revealed that ethanol-induced DRAM1 of hepatic cells could increase the PKM2-enriched EVs, promote macrophage activation, and aggravate the disease progression of ALD. These findings suggested that DRAM1 might be a potentially promising target for the therapy of ALD.

INTRODUCTION

DNA damage-regulated autophagy modulator 1 (DRAM1) is a transmembrane protein with six transmembrane domains that is mainly located in the lysosome.[1,2] As a p53 target gene, DRAM1 plays a key role in p53-dependent autophagy and apoptosis.[3] DRAM1-mediated mitophagy was a major apoptotic inducer during the progression of hepatic steatosis.[4] It was also reported that DRAM1 enhanced lipid accumulation in osteoporotic rats.[5] Additionally, DRAM1 was involved in oral inflammation and infection.[6] In view of the points above, DRAM1 could play important roles in inflammation, lipid accumulation, and hepatic apoptosis. Alcohol-related liver disease (ALD) is characterized by increased hepatic lipid accumulation, inflammation, and hepatic apoptosis. However, the role of DRAM1 during the progression of ALD remains unclear.

ALD has been one of the most common types of liver diseases worldwide, and it covers a range of diseases with different severities including simple fatty liver, alcoholic hepatitis (AH), fibrosis, and cirrhosis and its complications.[7,8] In addition, alcohol consumption has been a major risk factor for the global burden of disease.[8,9] Some current interventions such as corticosteroids, biological agents, and liver transplantation have been used for the treatment of ALD. However, the consensus for treatments for ALD has not been reached.[10–12] Based on the severity of ALD, it is urgent to seek for new targets for the diagnosis and treatment of ALD.

Alcohol could lead to the increase of gut permeability, where enteric gram-negative bacteria and enterogenic lipopolysaccharide (LPS) could migrate into portal circulation and transfer to the liver to activate the hepatic macrophages.[13–15] Hepatic macrophages are the largest population of innate immune cells in the liver and play a key role in maintaining liver function and homeostasis.[16] The inflammation induced by alcohol is mainly mediated by macrophages.[17] M1 macrophages could exert pro-inflammatory effects and release pro-inflammatory cytokines.[18,19]

Extracellular vesicles (EVs), mainly including ectosomes and exosomes, are natural nanometer-sized carriers.[20–22] EVs can be secreted by almost all cells and deliver proteins, lipids, and various nucleic acids from donor cells to both near and distant recipient cells.[21,22] EVs and their contents have been reported to be the potential biomarkers for the diagnosis and prognosis of diseases including

Received 27 August 2021; accepted 9 December 2021;
https://doi.org/10.1016/j.omtn.2021.12.017.

[4]These authors contributed equally

Correspondence: Likun Zhuang, Clinical Research Center, Qingdao Municipal Hospital, Qingdao University, Qingdao 266071 China.
E-mail: zlk0823@163.com
Correspondence: Yongning Xin, Clinical Research Center, Qingdao Municipal Hospital, Qingdao University, Qingdao 266071 China.
E-mail: xinyongning9812@163.com

ALD.[14,23,24] Previous study has shown that alcohol exposure could release CD40L-containing EVs from hepatocytes, which stimulated the activation of macrophages and led to inflammation in ALD.[14] However, the correlation between EVs and ALD progression still needs to be further investigated.

In this study, we investigated the expression, role, and mechanism of DRAM1 during the progression of ALD. Our results showed that DRAM1 knockout attenuated, and liver-specific DRAM1 overexpression aggravated, the alcohol-induced hepatic steatosis, injury, and expressions of M1 macrophage markers in mice. Mechanistical investigation showed that DRAM1 of hepatic cells could interact with pyruvate kinase M2 (PKM2) and mediate alcohol-induced secretion of PKM2 through extracellular vesicles, and the ectosomes released from hepatic cells with DRAM1 overexpression could promote macrophage activation. We also found that DRAM1 level was higher in liver tissues of patients with ALD and was positively associated with the levels of M1 macrophage markers. These data suggested that DRAM1 might be a potential marker for the diagnosis and a potential target for the treatment of patients with ALD.

RESULTS

Alcohol-induced increase of DRAM1 expression occurred in the early stage and was p53-dependent

To investigate the relationship between DRAM1 and ALD progression, firstly, we detected the expression and location of DRAM1 in liver tissues of mice fed with an ethanol diet. Wild-type (WT) mice were divided into two groups and were fed with an ethanol diet or control diet (Figure 1A). The results of immunofluorescence assays showed that DRAM1 was mainly co-localized with the hepatocyte marker cytochrome P450 family 2 subfamily E member 1 (CYP2E1) but not the macrophage marker F4/80 in liver tissues of both the control and ethanol groups, indicating that DRAM1 was mainly expressed in hepatic parenchymal cells (Figure 1B). At different time points (3 days, 1 week, 2 weeks, and 4 weeks) after ethanol feeding, the levels of DRAM1 in liver tissues of mice were measured. Our results showed that compared with mice fed with a control diet, DRAM1 level in liver tissues of mice fed with an ethanol diet was significantly increased at 3 days. In addition, DRAM1 expression was unchanged at 1 or 2 weeks, and even decreased at 4 weeks in liver tissues of mice fed with ethanol (Figure 1C). These results suggested that ethanol intake might induce an increase in DRAM1 expression in liver tissues of mice at the early stage.

At the same time, we also verified the relationship between alcohol treatment and DRAM1 expression in human hepatic cell lines including HepG2 and Huh7 cells. Our results showed that DRAM1 level in HepG2 cells was increased at relatively low concentration (80 mM) and short time (12 h) of ethanol treatment (Figures 1D and 1E). Meanwhile, DRAM1 was significantly elevated in 80 mM, 400 mM, and 12 h groups in Huh7 cells treated with ethanol (Figures 1F and 1G). These results also indicated that the early stage of alcohol induction could lead to increased DRAM1 level in hepatic cells.

DRAM1 could be induced by p53, so then we investigated the role of p53 in alcohol-induced expression of DRAM1. When HepG2 cells were treated with ethanol, the expression level of p53 protein was increased (Figure 1H). We also found that p53 knockdown significantly attenuated ethanol-induced increase in DRAM1 level, indicating that p53 could regulate alcohol-induced DRAM1 expression (Figure 1I). These data indicated that the increased DRAM1 level induced by alcohol was p53 dependent.

DRAM1 knockout attenuated alcohol-induced hepatic lipid accumulation, hepatic injury, and expressions of M1 macrophage markers in mice

To further investigate the role of DRAM1 in the pathogenesis of ALD, we used DRAM1-knockout (KO) mice for further analysis (Figure 2A). qRT-PCR and western blot were used to confirm the knockout of DRAM in liver tissues of mice (Figures 2B and 2C). Then the DRAM1-KO mice were fed with ethanol diet to establish the ALD model. Our results showed that there was no significant difference in body weight between WT and DRAM1-KO mice after ethanol feeding (Figure 2D), whereas the liver weight and liver-to-body weight ratio of mice were significantly reduced in ethanol-fed DRAM1-KO mice compared with that in ethanol-fed WT mice (Figures 2E and 2F). Next, we evaluated hepatic steatosis and injury in these mice. Figures 2G and 2H showed that both plasma and liver triglyceride (TG) levels in DRAM1-KO mice were significantly lower than WT mice after ethanol feeding. Similarly, the results of oil red O staining showed that the accumulation of fat in liver tissues of DRAM1-KO mice fed with ethanol was reduced compared with the WT mice fed with ethanol (Figure 2I). Furthermore, the results of hematoxylin and eosin (H&E) staining showed that the number and size of vacuoles in liver tissue of DRAM1-KO mice were obviously decreased compared with WT mice after ethanol feeding (Figure 2J). We further analyzed the activity scores, which reflected three aspects including hepatocyte steatosis, inflammatory cell infiltration, and hepatocyte ballooning degeneration. The results showed that the activity scores of liver tissues in WT mice were significantly higher than those in DRAM1-KO mice after ethanol feeding (Figure 2K). We also measured the levels of plasma alanine aminotransferase (ALT) activity and aspartate aminotransferase (AST), and the results showed that DRAM1-KO significantly reduced the level of ALT in plasma induced by ethanol (Figure 2L), although the knockout of DRAM1 did not change the level of plasma AST (Figure 2M).

The previous studies revealed that alcohol could induce the activation of hepatic macrophages.[25] To evaluate the number of macrophages in liver tissues of mice, the immunohistochemistry assay for F4/80 was used, and the results showed that ethanol feeding increased the number of macrophages in the livers of WT mice, whereas the ethanol-induced increase of macrophages was attenuated in DRAM1-KO mice (Figure 2N). Tumor necrosis factor alpha (TNF-α), interleukin-1β (IL-1β), and interleukin-6 (IL-6) were both M1 macrophage markers and pro-inflammatory cytokines. As shown in Figure 2O, the levels of TNF-α, IL-1β, and IL-6 in liver tissues of ethanol-treated DRAM1-KO mice were significantly lower

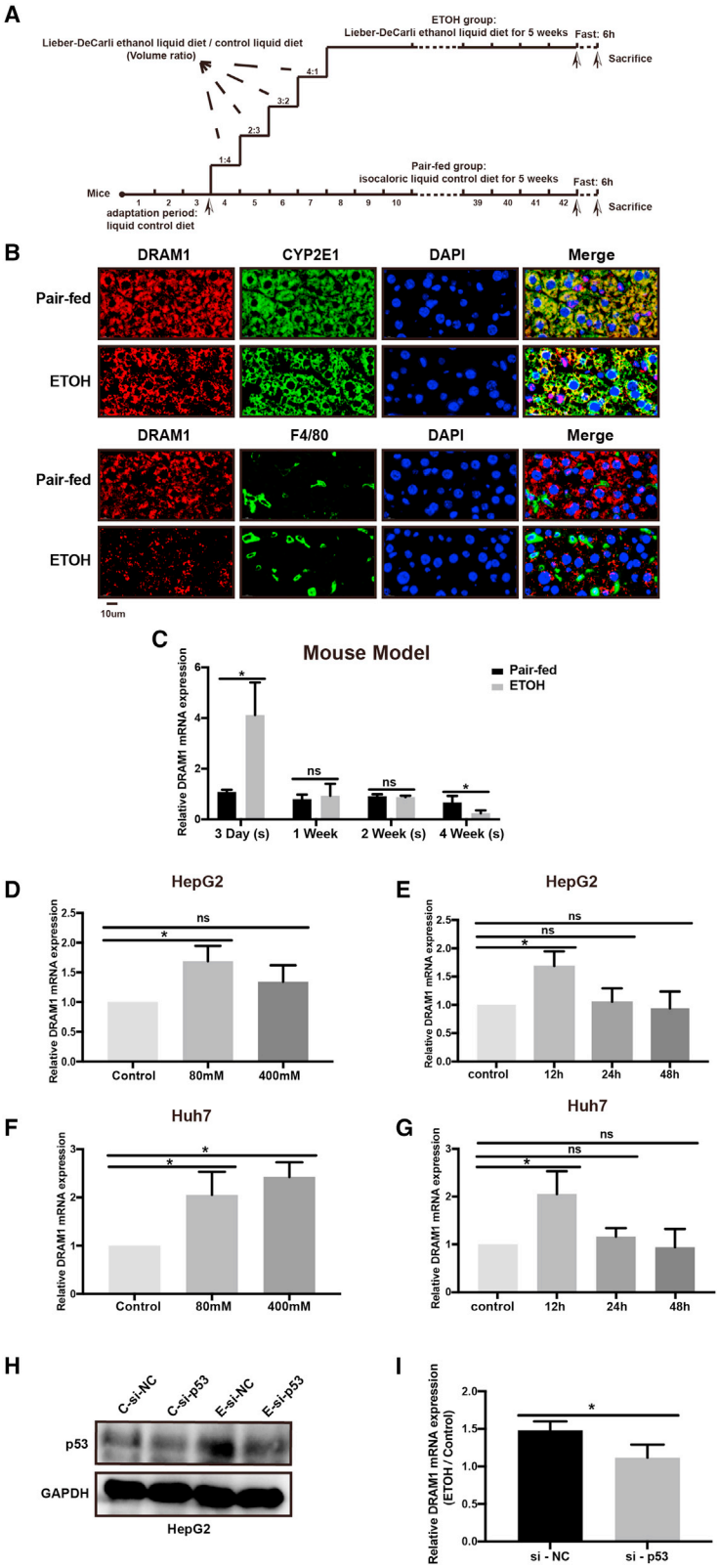

Figure 1. DRAM1 expressions in liver tissues of mice and hepatic cells with ethanol treatment

(A) Schematic diagram for the construction of mouse model of ALD. (B) Immunofluorescence assays of liver tissues in pair-fed and ethanol-fed mice were used to measure the expressions of DRAM1, CYP2E1, and F4/80 (Scale bars: 10μm). (C) Mice were fed with ethanol diet or control diet for 3 days, 1 week, 2 weeks, and 4 weeks, respectively. The expression levels of DRAM1 in liver tissues of mice were measured by qRT-PCR (n = 3–4). (D–G) HepG2 cells (D) and Huh7 cells (F) were treated with 80 mM or 400 mM ethanol for 12 h, and the levels of DRAM1 were measured by qRT-PCR. The levels of DRAM1 in HepG2 (E) and Huh7 cells (G) were measured by qRT-PCR after being treated with 80 mM ethanol for 12 h, 24 h, or 48 h. (H) Levels of p53 protein were detected by western blot in ethanol-treated HepG2 cells transfected with p53 siRNAs. (I) qRT-PCR was used to detect the mRNA level of DRAM1, and the ratio between the values of the ETOH-treated group and the control group was calculated. *$p < 0.05$; ns, no significance.

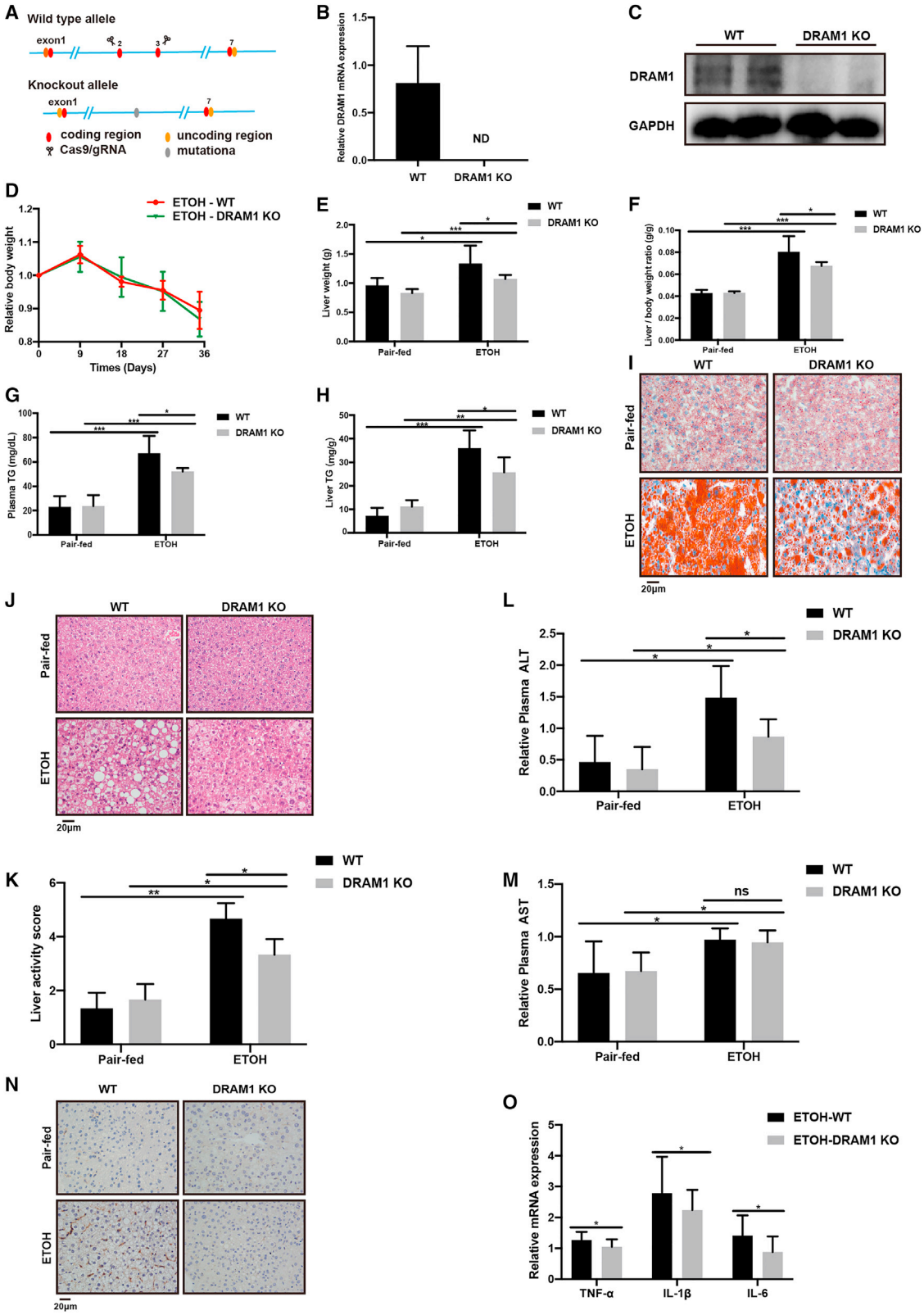

(legend on next page)

than those of ethanol-treated WT mice. Oxidative stress was also one of the key features of ALD, as ethanol and its metabolites can increase the production of reactive oxygen species and enhance the effect of peroxidation.[26] However, we found no significant difference in superoxide dismutase (SOD) and malondialdehyde (MDA) levels of liver tissues between the ethanol-treated WT and DRAM1-KO mice (Figure S1), which indicated that DRAM1 might not affect the ethanol-induced oxidative stress. Together, these observations suggested that DRAM1 deficiency could attenuated alcohol-induced hepatic steatosis, injury, and the expressions of M1 macrophage markers in mice.

Liver-specific DRAM1 overexpression enhanced ethanol-induced hepatic lipid accumulation, hepatic injury, and expressions of M1 macrophage markers in mice

In this study, we also used adeno-associated virus (AAV) to specifically overexpress DRAM1 in liver cells of mice. qRT-PCR and western blot assays were used to verify that DRAM1 was successfully overexpressed in liver (Figures 3A and 3B) but not overexpressed in other organs of mice (Figure S2). The AAV-vector and AAV-DRAM1^{Hep} mice were also fed with control diet and ethanol diet. The liver-specific DRAM1 overexpression did not affect the body weight of the ethanol-fed mice (Figure 3C), but the liver weight of the AAV-DRAM1^{Hep} mice fed with ethanol was significantly higher than that of the ethanol-treated AAV-vector mice (Figure 3D). Compared with AAV-vector mice after ethanol feeding, plasma and liver TG levels of AAV-DRAM1^{Hep} mice after ethanol feeding were also significantly increased (Figures 3E and 3F). The results of oil red O and H&E staining showed that liver-specific DRAM1 overexpression aggravated ethanol-induced hepatic lipid accumulation in liver tissues (Figures 3G and 3H). The activity scores of liver sections also showed that liver-specific DRAM1 overexpression significantly increased the liver activity score in ethanol-fed mice (Figure 3I). At the same time, ALT level in plasma was significantly higher in AAV-DRAM1^{Hep} mice fed with ethanol than that in AAV-vector mice after ethanol feeding, but no significant change was observed in plasma AST level between the two groups (Figures 3J and 3K). Furthermore, liver-specific DRAM1 overexpression significantly increased ethanol-induced macrophage number and the expressions of M1 macrophage markers including IL-1β and IL-6 (Figures 3L and 3M). These data suggested that liver-specific DRAM1 overexpression could significantly aggravate ethanol-induced hepatic steatosis, liver injury, and expressions of M1 macrophage markers.

Ectosomes released from DRAM1-overexpressed hepatic cells promoted macrophage activation

How did DRAM1, which was mainly expressed in hepatic parenchymal cells, affect macrophage activation? Phorbol 12-myristate 13-acetate (PMA) could induce human monocytic cell line THP-1 to macrophages, which can be verified by detecting the increase of CD68 expression (Figure S3). Interestingly, overexpression of DRAM1 did not affect PMA-induced differentiation and the expression of M1 macrophage marker CD86 in THP-1 cells (Figure 4A). However, when HepG2 cells with DRAM1 overexpression were co-cultured with THP-1 cells using a transwell chamber (Figures 4B and 4C), the dramatic morphological change of co-cultured THP-1 cells was observed, and the CD68 level was increased (Figures 4D and 4E). We also found that the culture supernatant from ethanol-treated HepG2 cells could promote PMA-induced differentiation and activation of THP-1 cells, and DRAM1 knockdown could attenuate the effects of ethanol (Figure 4F).

Studies have revealed that EVs including ectosomes and exosomes in the culture supernatant could play important roles in cellular communication.[21,27] Then we investigated the roles of EVs in the communications between DRAM1-overexpressing HepG2 cells and THP-1 cells. We used ultracentrifugation to isolate the ectosomes and exosomes in cell culture supernatant of HepG2 cells with DRAM1 overexpression (Figure 4G). The typical appearance of ectosomes and exosomes were respectively visualized under the transmission electron microscope (Figure 4H). The ectosome marker matrix metalloproteinase 2 (MMP2) and the exosome marker CD63 were also detected to confirm that there was no mutual contamination (Figure 4I). Next, we added ectosomes or exosomes derived from HepG2 cells with DRAM1 overexpression to the cell culture supernatant of THP-1 cells. We found that the adhesion ability was significantly upregulated in THP-1 cells incubated with ectosomes derived from HepG2 cells with DRAM1 overexpression compared with the cells transfected with empty vector, but the derived exosomes did not change the adhesion of THP-1 cells (Figure 4J). qRT-PCR and western blot also showed that the mRNA and protein level of CD68 were significantly increased in THP-1 cells incubated with ectosomes from HepG2 cells in DRAM1 overexpression group (Figures 4K and 4M), while the mRNA and protein expression of CD68 were unchanged between the THP-1 cells incubated with exosomes from the HepG2 cells transfected with DRAM1 expression plasmid and empty vector (Figure 4L, N). In addition, we found that when ectosomes derived from HepG2 cells overexpressing DRAM1 were incubated with PMA-treated THP-1 cells, the levels of M1 macrophage markers,

Figure 2. Ethanol-induced hepatic lipid accumulation, hepatic injury, and expressions of M1 macrophage markers in DRAM1-knockout mice

(A) CRISPR/cas9 technology was used to knockout the DRAM1 gene in mice. (B and C) DRAM1 levels in liver tissues of DRAM1-KO mice were measured by qRT-PCR (B) and western blot (C). (D–O) WT and DRAM1-KO mice (n = 4–6) were fed with ethanol diet or control diet for five weeks. Body weight (D), liver weight (E), liver-to-body weight ratio (F), plasma TG levels (G), liver tissue TG levels (H), oil red O staining (I), H&E staining (J), liver activity score (K), plasma ALT levels (L), plasma AST levels (M), immunohistochemistry staining for F4/80 (N), and the mRNA levels of TNF-α, IL-1β, and IL-6 in liver tissues (O) were measured. Images were captured for oil red O staining, H&E staining, and F4/80 immunohistochemistry staining at 400× magnification (Scale bars: 20μm). *p < 0.05; **p < 0.01; ***p < 0.001; ns, no significance; ND, no detection.

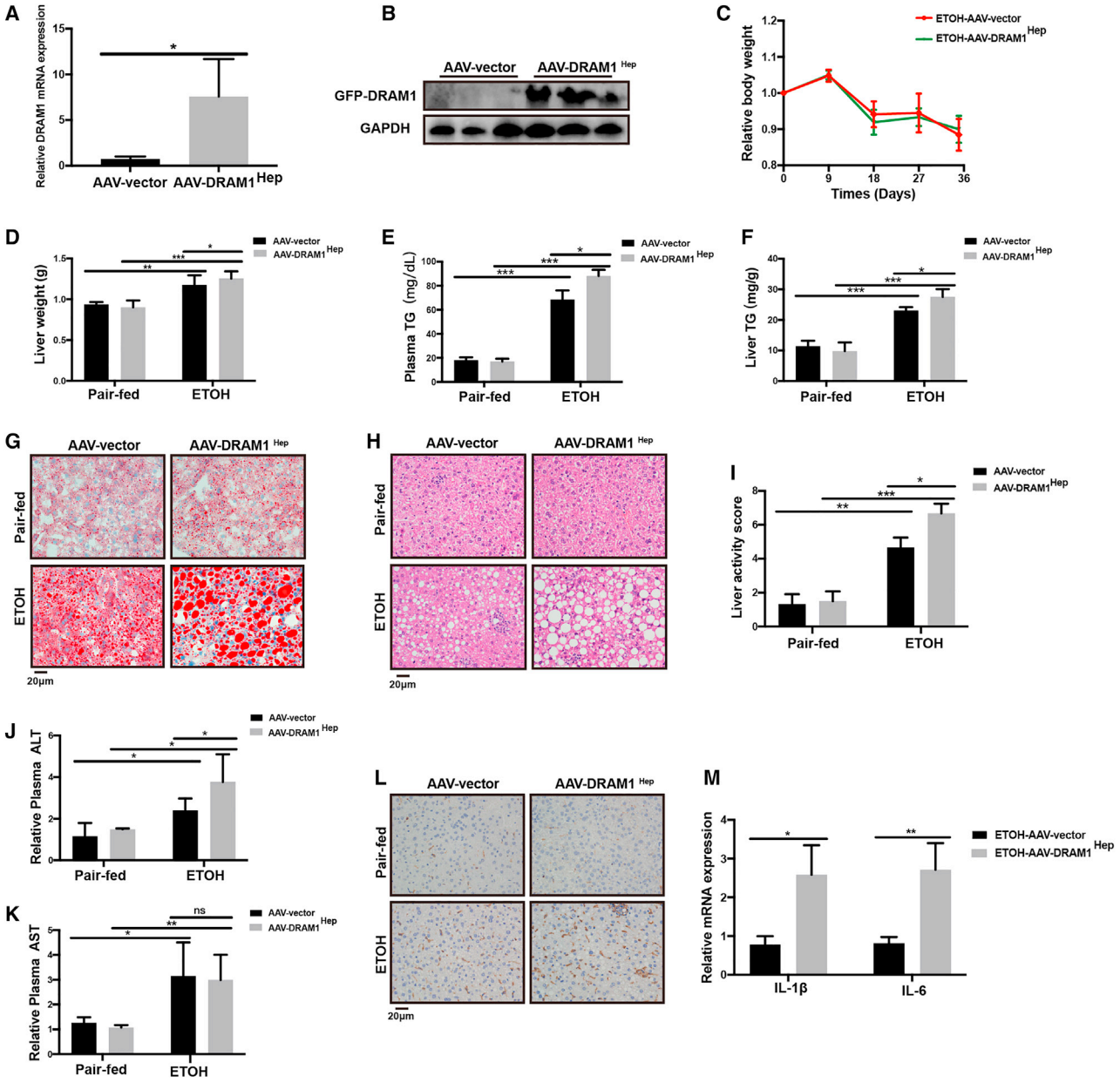

Figure 3. Ethanol-induced hepatic lipid accumulation, hepatic injury, and expressions of M1 macrophage markers in mice with liver-specific overexpression of DRAM1

(A) DRAM1 levels of liver tissues in AAV-vector and AAV-DRAM1^{Hep} mice were measured by qRT-PCR. (B) Western blot assay for GFP tag in liver tissues of AAV-vector and AAV-DRAM1^{Hep} mice. (C–M) AAV-vector and AAV-DRAM1^{Hep} mice (n = 3–5) were fed with ethanol diet or control diet for 5 weeks. Body weight (C), liver weight (D), plasma TG levels (E), TG levels of liver tissues (F), oil red O staining (G), H&E staining (H), liver activity score (I), plasma ALT levels (J), plasma AST levels (K), immunohistochemistry staining for F4/80 (L), and the mRNA levels of IL-1β and IL-6 in liver tissues (M) were measured. Images were captured for oil red O staining, H&E staining, and F4/80 immunohistochemistry staining at 400× magnification (Scale bars: 20μm). *p < 0.05; **p < 0.01; ***p < 0.001; ns, no significance.

including TNF-α, IL-1β, IL-6, and monocyte chemo attractant protein 1 (MCP-1), were significantly increased (Figure 4O). Together, these observations suggest that ectosomes released from hepatic cells with DRAM1 overexpression could promote the differentiation and activation of macrophages.

Alcohol-induced DRAM1 of hepatic cells increased the PKM2 level in secreted extracellular vesicles

It has been reported that PKM2 in ectosomes can promote the differentiation of THP-1 cells into macrophages.[28] We further analyzed the expression level of PKM2 in plasma EVs of mice fed with ethanol. The

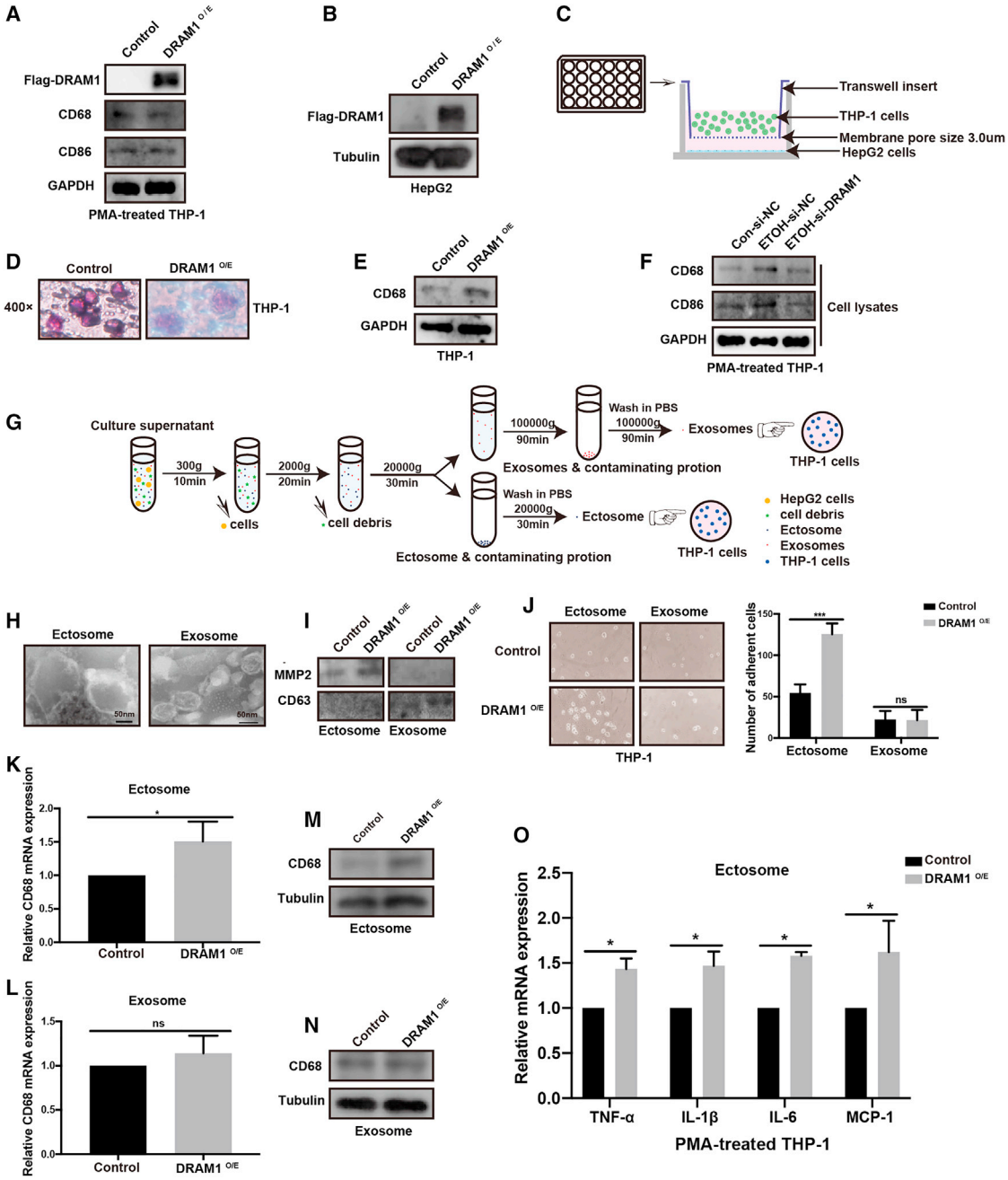

Figure 4. Ectosomes from hepatic cells overexpressing DRAM1 regulated the differentiation and activation of macrophages

(A) Flag-DRAM1 was overexpressed in PMA-treated THP-1 cells, and the protein levels of CD68 and CD86 were detected by western blot. (B) HepG2 cells were transfected with the Flag-DRAM1 expression plasmids, and the level of Flag-DRAM1 was detected by western blot. (C) HepG2 cells in the lower plate were transfected with Flag-DRAM1 expression plasmids, and the THP-1 cells were placed in the upper chamber. The two cells were co-cultured in a transwell chamber. (D–E) The morphological images (D) and CD68 protein level (E) of co-cultured THP-1 cells were detected. (F) The culture supernatant of HepG2 cells transfected with the corresponding siRNAs were incubated with PMA-incubated THP-1 cells. The protein levels of CD68 and CD86 in PMA-treated THP-1 cells were detected by western blot. (G) Ultracentrifugation was used to isolate the ectosomes and exosomes in the culture supernatant of HepG2 cells transfected with Flag-DRAM1 expression plasmids or empty vector. (H) The typical pictures of ectosomes and exosomes were respectively visualized under the transmission electron microscope. (I) The ectosome marker MMP2 and the exosome marker CD63 were detected by western blot. (J–N) Ectosomes or exosomes extracted from the culture supernatants of HepG2 cells transfected with Flag-DRAM1 expression plasmids or empty

(legend continued on next page)

results showed that ethanol feeding increased the level of PKM2 in plasma EVs of mice, and DRAM1 knockout attenuated the increase of PKM2 level induced by ethanol (Figure 5A). Meanwhile, liver-specific DRAM1 overexpression also increased the level of PKM2 in plasma EVs of mice fed with ethanol (Figure 5B). Immunofluorescence analysis showed that both ethanol and liver-specific DRAM1 overexpression could increase the proportion of macrophages in PKM2-positive cells of liver tissues in mice (Figures 5C and 5D). The *in vitro* experiments also showed that overexpression of DRAM1 in HepG2 cells could lead to an increase of PKM2 in EVs and co-cultured THP1 cells treated with PMA (Figures 5E and 5F). Interestingly, overexpression of PKM2 in PMA-treated THP-1 cells resulted in a significant increase in CD68 and CD86 levels, which indicated that PKM2 could promote the M1 macrophage activation (Figure 5G). In addition, we found that ethanol could increase the levels of DRAM1 and PKM2 in EVs from HepG2 cells, while DRAM1 knockdown could attenuate the effects of ethanol (Figure 5H). Furthermore, ultracentrifugation was used to isolate ectosomes and exosomes from the cell culture supernatant of HepG2 cells with DRAM1 overexpression, and we found that PKM2 was only increased in ectosomes but not in exosomes of DRAM1-overexpressed group (Figure 5I). When PMA-treated THP-1 cells were incubated with ectosomes or exosomes, it was found that PKM2 level was increased in PMA-treated THP-1 cells incubated with ectosomes from DRAM1-overexpressed group, while there was no difference of the PKM2 level in PMA-treated THP-1 cells between the two groups incubated with exosomes (Figure 5J). In summary, our results suggested that DRAM1 in hepatic cells could promote the level of PKM2 in EVs.

DRAM1 interacted with PKM2 and promoted its plasma membrane localization in hepatic cells

The above experiments showed that both DRAM1 and PKM2 expression were detected in EVs. Then we investigated whether DRAM1 could interact with PKM2. Using co-immunoprecipitation (coIP) assay, we verified the interaction between DRAM1 and PKM2 (Figure 6A). In addition, the results of immunofluorescence also revealed that DRAM1 and PKM2 were co-localized in HepG2 cells and liver tissues of mice (Figures 6B and 6C). Considering that DRAM1 can be located in lysosomes and plasma membrane, we further investigated whether DRAM1 could affect the localization of PKM2 in hepatic cells. We overexpressed DRAM1 in HepG2 cells and extracted the proteins from lysosomes, plasma membrane, and cytoplasm. Our results showed that the expression of PKM2 was significantly increased in both lysosomes and plasma membrane, whereas there was almost no change in the cytoplasm (Figure 6D). These data suggested that DRAM1 could interact with PKM2 and promote its plasma membrane localization in hepatic cells.

DRAM1 expression was upregulated in liver tissues of ALD patients and was positively correlated with M1 macrophage markers

To explore the expression of DRAM1 in liver tissues of ALD patients, we analyzed 21,654 gene expressions in liver tissues of AH patients and the controls from a cDNA microarray (GEO database: GSE28619). The results showed a significant increase of DRAM1 expression in liver tissues of AH patients compared to controls (Figure 7A). In this dataset, 6,035 genes showed significant correlations with DRAM1 ($p < 0.05$), 3,619 genes were positive correlated ($p < 0.05$, correlation coefficient ≥ 0.3), and 2,416 genes were negative correlated ($p < 0.05$, correlation coefficient ≤ -0.3). The expression level of DRAM1 in liver tissues was positively correlated with the expression levels of M1 macrophage markers including CD86, C-X-C motif chemokine ligand 9 (CXCL9), C-X-C motif chemokine ligand 10 (CXCL10), and Toll-like receptor 2 (TLR2) (Figure 7B), but not positively correlated with the levels of M2 macrophage markers including CD163, interleukin-10 (IL-10), arginase-1 (Arg1), and CD209 (Figure 7C). Then the samples were divided into two groups including the DRAM1-low expression group and DRAM1-high expression group based on the cutoff value. The results showed that levels of the M1 macrophage markers CXCL9, CXCL10, and TLR2 were significantly increased in DRAM1-high expression group compared with that in DRAM1-low expression group (Figure 7D), while the levels of the M2 macrophage markers CD163, Arg1, and CD209 were not significantly changed (Figure 7E). Furthermore, compared with the control group, the expression levels of p53 and PKM2 in liver tissues of AH patients were significantly increased (Figures 7F and 7H). There was also a significant positive correlation between DRAM1 and p53 or PKM2 (Figures 7G and 7I). Similar results were also shown in another RNA sequencing dataset (GEO database: GSE155907) of liver tissues in AH patients and controls (Figure S4). These findings indicated that DRAM1 expression was significantly elevated in liver tissues of ALD patients and was positively associated with the expressions of M1 macrophage markers.

DISCUSSION

DRAM1 was revealed to be involved in the occurrence and development of a variety of diseases.[3,6,29,30] In this study, we analyzed the data from the GEO database and found that DRAM1 was significantly elevated in liver tissues of patients with ALD. More interestingly, our analysis showed that DRAM1 expression of liver tissues was positively correlated with the expressions of M1 macrophage markers. Further *in vivo* and *in vitro* experiments indicated that DRAM1 expression of hepatic cells was increased significantly at the early stage after ethanol treatment. These results suggested that DRAM1 expression in liver tissues might be a potential biomarker for the occurrence of ALD. It has been reported that serum deprivation or hepatic

vector were respectively added into the culture medium of THP-1 cells. The adhesion of THP-1 cells was observed and counted in each group (J). The mRNA and protein levels of CD68 in THP-1 cells incubated with ectosomes or exosomes (K–N). (O) Ectosomes extracted from the culture supernatants of HepG2 cells transfected with Flag-DRAM1 expression plasmids or empty vector were incubated with PMA-treated THP-1 cells. The mRNA levels of M1 macrophage markers, including TNF-α, IL-1β, IL-6, and MCP-1, were detected by qRT-PCR. *$p < 0.05$; ***$p < 0.001$; ns, no significance.

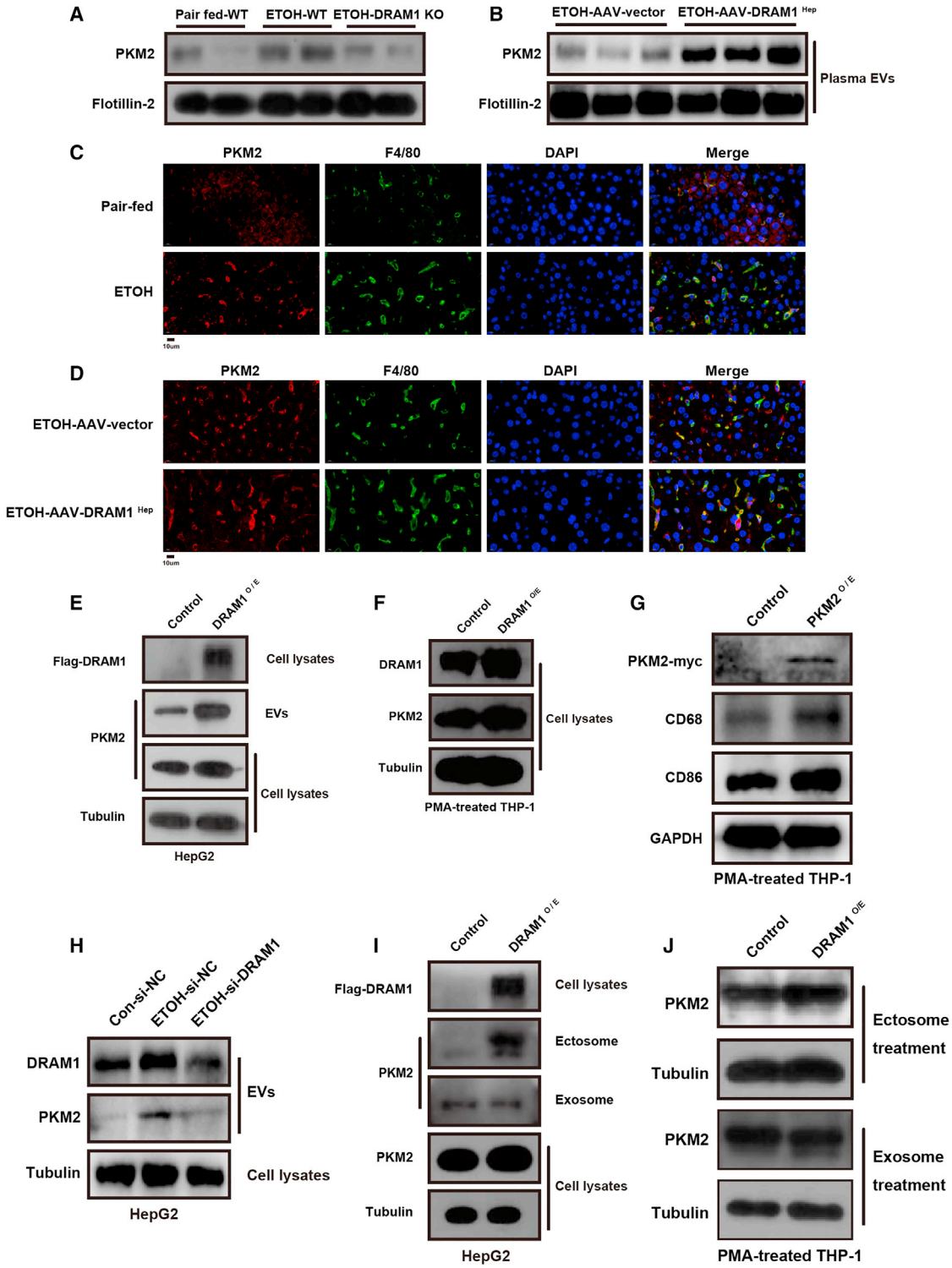

Figure 5. DRAM1 regulated PKM2 level in extracellular vesicles released from hepatic cells

(A) EVs were extracted from the plasma of WT or DRAM1-KO mice fed with control or ethanol diet. Protein level of PKM2 in EVs were detected by western blot. (B) EVs were extracted from the plasma of AAV-vector and AAV-DRAM1^{Hep} mice fed with ethanol. Protein level of PKM2 in EVs was detected by western blot. (C) Immunofluorescence assays of liver tissues in control and ethanol-fed mice were used to measure the expressions of PKM2 and F4/80 (Scale bars: 10μm). (D) Immunofluorescence assays of liver

(legend continued on next page)

ischemia could induce DRAM1 expression of hepatocytes, and DRAM1 overexpression could increase the ischemia-induced liver injury.[29,31] Moreover, DRAM1-mediated autophagy and apoptosis might be critical in high-fat-diet-induced mild steatosis of liver tissues.[4] In this study, mouse model experiments showed that DRAM1 knockout could reduce, and liver-specific DRAM1 overexpression could promote, ethanol-induced liver steatosis, liver injury, and expressions of M1 macrophage markers. Therefore, DRAM1 might also be a potential target for hepatic steatosis and inflammation during the progression of ALD. In future study, we would try to use some intervention methods such as RNA silencing to evaluate the therapeutic potential of inhibiting DRAM1 in ALD.

In this study, we revealed that DRAM1 level in liver tissues of mice fed with an ethanol diet was significantly increased at 3 days, not significantly changed at 1 or 2 weeks, and even decreased at 4 weeks (Figure 1C). Two points should be considered for the preceding results. Firstly, there were about 4 days of adaptative period for ethanol liquid diet before the construction of the ALD mouse model. Actually, we and other groups revealed that mild hepatic steatosis, inflammation, and injury could be observed for a few days after the construction of an ALD mouse model.[32,33] We found that the level of DRAM1 in liver tissues of mice fed with an ethanol diet was significantly increased at 3 days and was relatively high, though not significantly, at 1 week. These data suggested that the level of DRAM1 was evaluated at the early stage during ethanol-induced hepatic steatosis, injury, and inflammation. Secondly, DRAM1 could be induced by p53, which is a regulator of cellular responses to stresses such as chemotherapy agents, hypoxia, fatty acid, and alcohol.[34–37] p53 can also play different or even opposite roles in different stages of nonalcoholic fatty liver disease (NAFLD) and with different drugs for cancer therapies.[38,39] In this study, we also revealed that the expression of p53 was positively correlated with DRAM1 in ALD patients, and p53 could regulate alcohol-induced expression of DRAM1. In future study, we would investigate whether DRAM could play different roles in different stages of ALD.

Our mechanistic investigations showed that DRAM1 overexpression could increase the level of PKM2 in EVs released from hepatic cells. PKM2 is a key enzyme that regulates cell metabolism and growth by catalyzing the conversion of phosphoenolpyruvate into pyruvate and providing ATP in the glycolysis pathway.[40,41] It has been found that overexpression of PKM2 led to increased lipid accumulation in hepatic cancer cells treated with palmitate.[40] PKM2 expression was strongly increased in LPS-activated macrophages and is a key regulator of IL-1β production, macrophage polarization, glycolysis reprogramming, and Warburg metabolism in LPS-activated macrophages.[42,43] Recent studies have shown that PKM2 expression was increased in the serum of severely obese people, and the level of PKM2 was higher in liver tissues of non-alcoholic steatohepatitis (NASH) patients.[44] In view of these facts, PKM2 might be related with steatohepatitis and inflammation in the liver. EVs are implicated in cell-cell communication, and secretory PKM2 expression has been identified in ectosomes.[27,45] It was revealed that ectosomal PKM2 can induce macrophage differentiation.[28] In this study, our results also showed that ectosomes isolated from the cell culture supernatant of hepatic cells with DRAM1 overexpression could promote the activation of PMA-treated THP-1 cells, which might be caused by the transfer of PKM2 protein from the DRAM1-overexpressed hepatic cells to THP-1 cells by ectosomes.

DRAM1 is a membrane protein and mainly located in lysosomes and plasma membrane. In this study, it was revealed that DRAM1 could interact with PKM2. Furthermore, overexpression of DRAM1 in hepatic cells resulted in the increased level of PKM2 in both lysosomes and plasma membrane. A previous study had shown that sumoylation of PKM2 could induce its translocation to plasma membrane and be sorted into the ectosomes by interacting with ARRDC1.[28] Here, our study also suggested that DRAM1 might be one of the factors that could recruit PKM2 to the plasma membrane and promote the secretion of PKM2 through EVs. In addition, the role of the increased PKM2 level in lysosomes after DRAM1 overexpression in hepatic cells would also be explored in our future study.

In summary, there was a significant increase of DRAM1 expression in ethanol-treated mouse liver and hepatic cells at the early stage. Liver-specific overexpression of DRAM1 in mice aggravated liver steatosis, liver injury, and the release of pro-inflammatory factors induced by ethanol feeding. Besides, ethanol-induced DRAM1 could help recruit PKM2 to the plasma membrane and increase the secretion of PKM2-enriched EVs from hepatic cells, and the EVs from hepatic cells with DRAM1 overexpression could promote the activation of macrophages (Figure 8). Our findings indicated that DRAM1 might be a modulator of the pathogenesis of ALD, and strategies aiming at inhibiting the expression of DRAM1 might have therapeutic potential for patients with ALD.

MATERIALS AND METHODS

Mouse model for ethanol feeding

Female mice, 6–8 weeks old, were selected to receive the Lieber-DeCarli ethanol liquid diet (5% v/v, 28% ethanol-derived calories), and the mice in control group were fed with isocaloric liquid diet (TROPHIC Animal Feed High-Tech, Jiangsu, China). At the end of

tissues in AAV-vector and AAV-DRAM1^{Hep} mice fed with ethanol were used to measure the expressions of PKM2 and F4/80 (Scale bars: 10μm). (E) Protein levels of PKM2 in EVs and cell lysates of hepG2 cells with DRAM1 overexpression were detected by western blot. (F) The culture supernatant of HepG2 cells transfected with the Flag-DRAM1 expression plasmids were incubated with PMA-incubated THP-1 cells. The expressions of both DRAM1 and PKM2 in PMA-treated THP-1 cells were detected by western blot. (G) PKM2-myc plasmids were transfected into PMA-treated THP-1 cells, and the protein levels of CD68 and CD86 were detected by western blot. (H) Ethanol-treated HepG2 cells were transfected with DRAM1 siRNAs and the EVs were isolated. The protein levels of DRAM1 and PKM2 in EVs were detected by western blot. (I–J) By ultracentrifugation, ectosomes and exosomes were extracted from the culture supernatants of HepG2 cells transfected with Flag-DRAM1 expression plasmids or empty vector and were added into the culture medium of PMA-treated THP-1 cells. Protein level of PKM2 in ectosomes, exosomes, and cell lysates of HepG2 cells were detected by western blot (I). PKM2 levels in PMA-treated THP-1 cells incubated with the corresponding ectosomes or exosomes were detected by western blot (J).

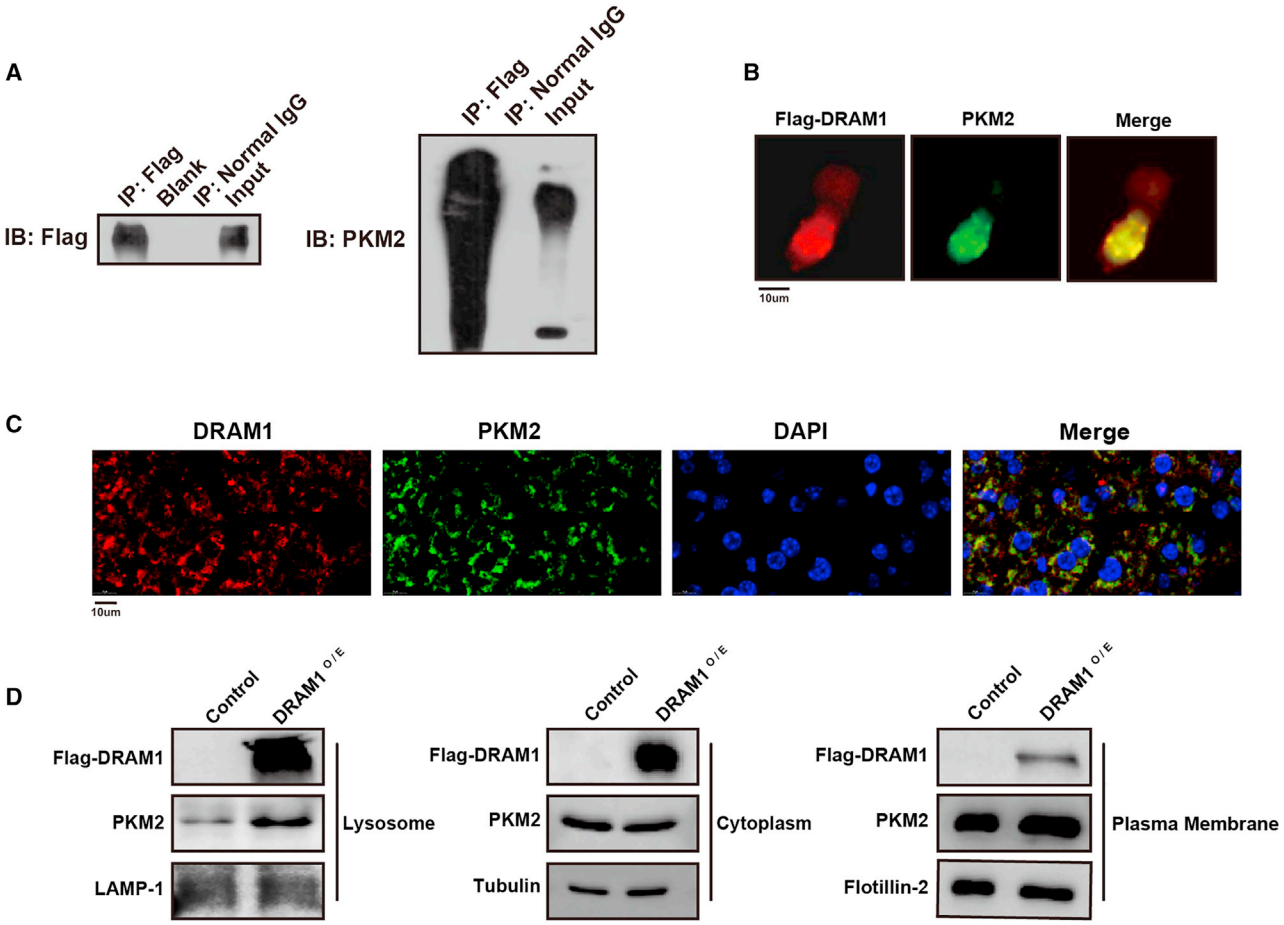

Figure 6. DRAM1 interacted with PKM2 and regulated its plasma membrane localization in hepatic cells

(A) coIP assay was conducted in cell lysates from HepG2 cells transfected with Flag-DRAM1 and PKM2-myc expression plasmids using anti-Flag antibody. Levels of Flag-DRAM1 and PKM2 were measured by western blot. (B) Immunofluorescence for Flag-DRAM1 and PKM2 in HepG2 cells transfected with Flag-DRAM1 expression plasmids (Scale bars: 10μm). (C) Immunofluorescence assays of liver tissues in WT mice were used to measure the expressions of DRAM1 and PKM2 (Scale bars: 10μm). (D) Protein levels of Flag-DRAM1 and PKM2 were detected in plasma membrane, lysosomes, and cytoplasm of HepG2 cells transfected with Flag-DRAM1 expression plasmids.

the treatment, mice were sacrificed after 6 h of fasting. Blood and liver tissues were collected for further analysis. The mice were bred under a 12-h light/dark cycle. All animal procedures were approved by the ethics committee of Experimental Research, Qingdao University.

DRAM1 knockout mice

C57BL/6 mice with DRAM1 gene knockout were obtained using the Clustered Regularly Interspaced Short Palindromic Repeats (CRISPR)/Cas9 technology (Shanghai Model Organisms Center, Shanghai, China). WT mice and homozygous type mice were obtained by the mating of heterozygous-type mice, and the genotypes were determined by PCR assays.

Mouse model with liver-specific DRAM1 overexpression

AAV was used to specifically overexpress DRAM1 in liver cells of mice. Female C57BL/6 mice (6–7 weeks old) were injected with either AAV-vector carrying DRAM1 gene (pAAV-ApoE/hAATp-DRAM1) or negative control vector (pAAV-ApoE/hAATp-null) (Shanghai Genechem, Shanghai, China) via tail vein injection. At 2 weeks after AAV injection, mice with liver-specific DRAM1 overexpression and controls were fed with ethanol liquid diet and control liquid diet.

Cell culture

HepG2, Huh7, and THP-1 cells were purchased from Shanghai Genechem. STR profiling and mycoplasma contamination testing of the cells were provided from Shanghai Genechem. Cells were cultured in an incubator with 5% CO_2 at 37°C. HepG2 and Huh7 cells were routinely maintained in Dulbecco's minimal essential medium (Biological Industries, Bet Haemek, Israel) supplemented with 10% fetal bovine serum (Biological Industries), and THP-1 cells were cultured in Roswell Park Memorial Institute 1640 medium (Biological Industries) containing 10% fetal bovine serum. For the isolation of EVs from the culture supernatant, cells were cultured in the Exo-Clear Cell Growth Medium (System Biosciences, Mountain View, CA,

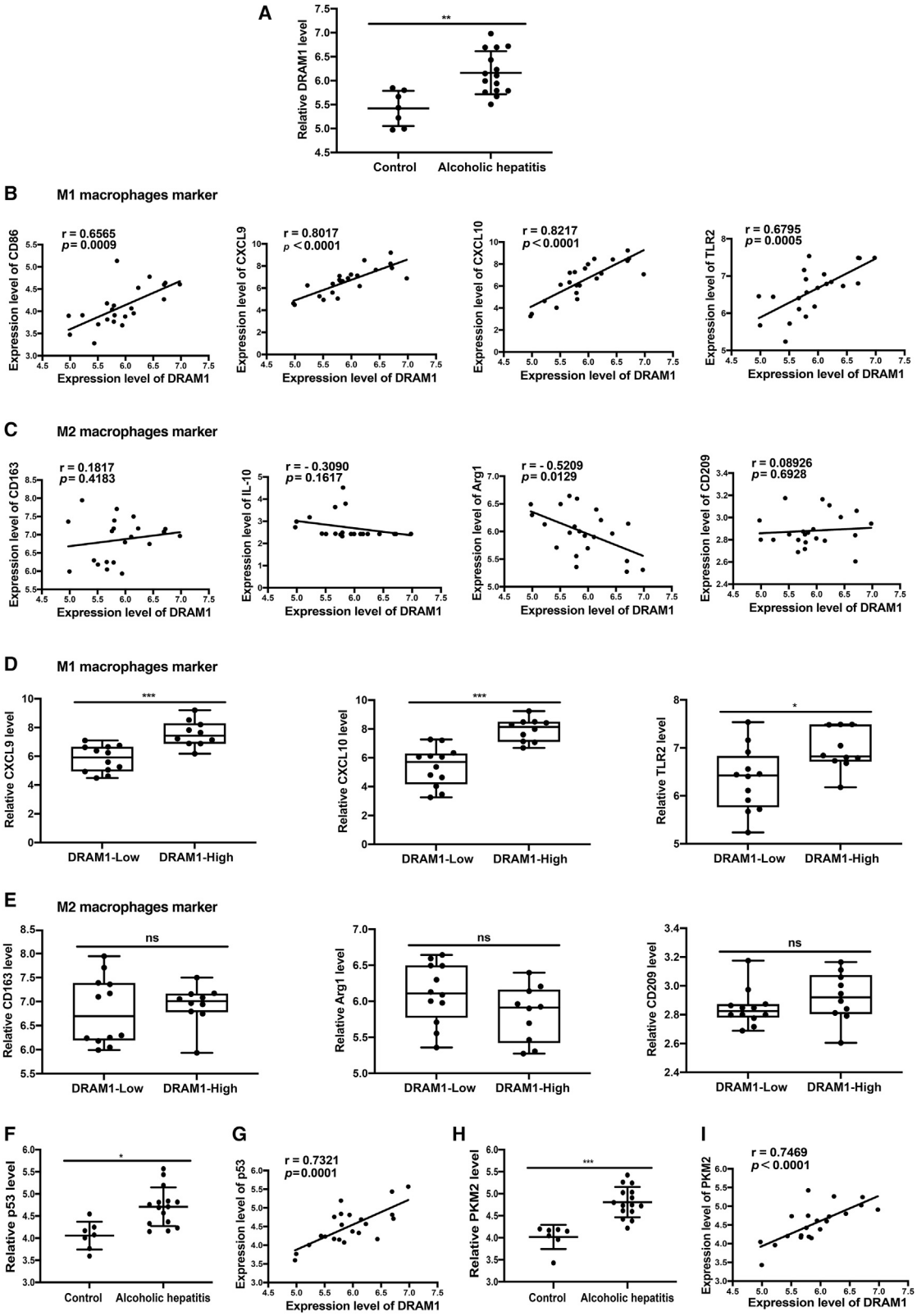

(legend on next page)

USA). HepG2 and Huh7 cells were treated with ethanol (Sinopharm Chemical Reagent, Shanghai, China) for subsequent experiments. Macrophage-like THP-1 cells were induced by phorbol 12-myristate 13-acetate (PMA, MedChemExpress, Monmouth Junction, NJ, USA).

Plasmid and oligonucleotide transfection

The plasmids encoding the DRAM1 gene with the FLAG tag and the PKM2 gene with the Myc tag were constructed. Lipofectamine 3000 Transfection Reagent (Invitrogen, Carlsbad, CA, USA) was applied for the transfection of plasmids. Small interfering RNAs (SiRNAs) targeting the human DRAM1 and p53 coding sequences were synthesized from Genepharma (Shanghai, China). Hiperfect transfection reagent (QIAGEN, Hilden, Germany) was applied for the transfection of siRNAs.

Quantitative real-time PCR

Total RNA was extracted from cells or liver tissues using RNAiso Plus reagent (TaKaRa, Shiga, Japan). The reverse-transcription was conducted using PrimeScript RT Reagent Kit with gDNA Eraser (TaKaRa). Then real-time PCR was performed using SYBR Green PCR Kit (QIAGEN), and relative gene expression was further calculated by ΔΔCt method. β-Actin or 18S rRNA was used as the internal control. Primers used in this study were synthesized from Beijing Genomics Institute (Shenzhen, China), and the sequences are listed in Table S1.

Western blot

Whole cell lysates were extracted using RIPA buffer (Solarbio, Beijing, China) supplemented with protease inhibitor cocktail (Sigma-Aldrich, St. Louis, MO, USA) and phosphatase inhibitor phenylmethylsulfonyl fluoride (Solarbio). Lysosomal and cytoplasmic protein were prepared using Lysosome Isolation Kit (GenMed Scientifics, USA). Plasma Membrane Protein Extraction Kit (Abcam, Cambridge, MA, USA) was used to extract the plasma membrane protein. Protein samples were separated in 10%–12% SDS-PAGE gel and transferred onto the hydrophobic polyvinylidene fluoride membrane (Millipore, Billerica, MA, USA). Indicated primary antibodies and horseradish-peroxidase-conjugated secondary antibodies are listed in Table S2. The protein band was detected using ECL reagent (Millipore) and then visualized by CHAMPCHEMI™ Chemiluminescent Imaging System (Sage Creation, Beijing, China).

Biochemical assays

TG level, ALT activity, and AST activity in the plasma of mice were determined using related commercial kits following the manufacturer's manuals (Jiancheng Bioengineering Institute, Nanjing, China). Besides, SOD and MDA in liver tissues of mice were measured using the corresponding kits (Jiancheng Bioengineering Institute). The OD values were measured using a spectrophotometer (Thermo Fisher Scientific, Waltham, MA, USA).

Oil red O staining, hematoxylin and eosin staining, Wright's staining, and immunohistochemistry

Liver tissue samples were fixed in 4% paraformaldehyde (Solarbio). Paraffin-embedded live tissue sections were used for H&E staining and immunohistochemistry for F4/80 antibody (GB11027, Servicebio, Wuhan, China). Frozen liver tissue sections were used for oil red O staining. THP-1 cells were stained with Wright's staining solution according to the manufacturer's instructions (Solarbio). The images were viewed and captured using an Olympus BX53 biomicroscope equipped with a DP26 digital imaging system (Olympus, Tokyo, Japan).

Extraction of extracellular vesicles by polymer-based precipitation

EVs in 100 μL plasma per mouse were isolated using Exosome Precipitation Kit (System Biosciences) according to the instruction. Besides, EVs in the cell culture supernatant were extracted using ExoQuick-TC Tissue Culture Media Exosome Precipitation Solution (System Biosciences).

Separation of ectosomes and exosomes by ultracentrifugation

Ectosomes and exosomes were isolated by ultracentrifugation. Culture supernatant of cells was firstly collected and centrifuged twice to remove the cells (300 g, 10 min, 4°C) and cell debris (2000 g, 20 min, 4°C). Ectosomes were isolated by ultracentrifugation at 20,000 g for 30 min, and then exosomes were isolated by ultracentrifugation at 100,000 g for 90 min. The pellets of exosomes or ectosomes obtained were resuspended in phosphate-buffered saline (Solarbio).

Co-cultivation in a transwell chamber

The co-cultivation was conducted using a 24-well transwell chamber with a membrane pore size of 3.0 μm (Corning Incorporated, Corning, NY, USA). HepG2 cells were cultured in the lower plate, and THP-1 cells were cultured in the upper chamber. The two cells were separated by the membrane of the transwell chamber.

Electron microscope

Ectosomes and exosomes were suspended in phosphate-buffered saline, spread onto a formvar/carbon-coated copper grid (Electron Microscopy Sciences, Hatfield, PA, USA), and stained with 3% aqueous

Figure 7. DRAM1 expression in liver tissues of AH patients

Dataset (GEO database: GSE28619) of AH patients and normal controls were analyzed. (A) DRAM1 levels in liver tissues of AH patients and controls were analyzed. The adjusted p value was calculated. (B) Pearson correlation analysis was used to analyze the correlations between DRAM1 level and M1 macrophage markers including CD86, CXCL9, CXCL10, and TLR2. (C) Pearson correlation analysis was used to analyze the correlations between DRAM1 level and M2 macrophage markers including CD163, IL-10, Arg1, and CD209. (D) The expression levels of CXCL9, CXCL10, and TLR2 in the DRAM1-high expression group and DRAM1-low expression group. (E) The expression levels of CD163, Arg1, and CD209 in the DRAM1-high expression group and DRAM1-low expression group. (F) p53 levels in liver tissues of AH patients and controls were analyzed. The adjusted p value was calculated. (G) Pearson correlation analysis was used to analyze the correlation between the DRAM1 and p53 level. (H) PKM2 levels in liver tissues of AH patients and controls were analyzed. The adjusted p value was calculated. (I) Pearson correlation analysis was used to analyze the correlation between DRAM1 level and PKM2 level. *$p < 0.05$; **$p < 0.01$; ***$p < 0.001$; ns, no significance.

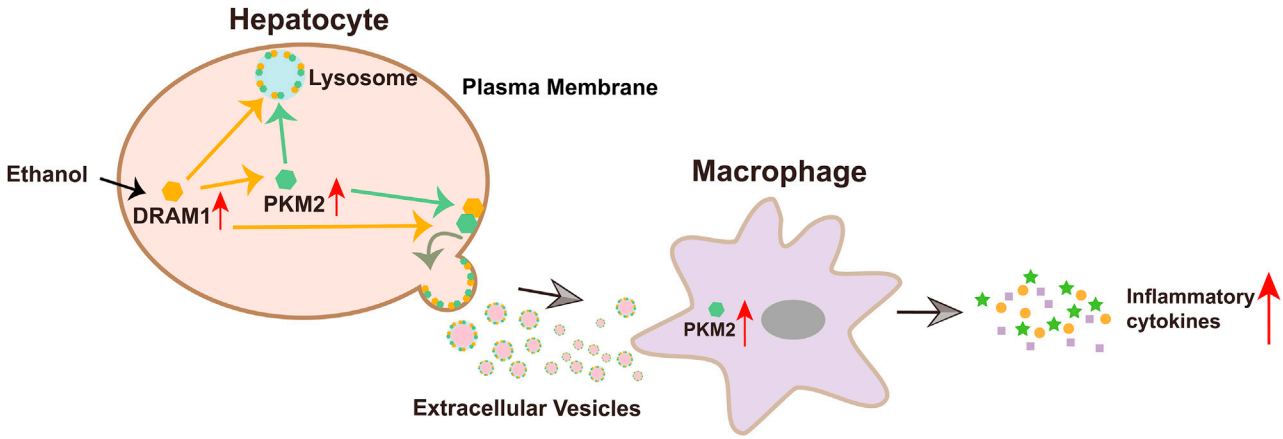

Figure 8. Diagram for the expression, role, and mechanism of DRAM1 in ethanol-treated hepatic cells

Ethanol can upregulate the expression of DRAM1 in hepatic cells at the early stage. DRAM1 further interacts with PKM2, promotes the translocation of PKM2 to the plasma membrane, and increases the secretion of PKM2-enriched EVs. Then the released EVs can promote macrophage activation and the expression of M1 macrophage markers.

phosphotungstic acid. The grids were observed and imaged using a JEM-1200EX transmission electron microscope (JEOL, Tokyo, Japan).

Co-immunoprecipitation

HepG2 cells were transfected and the total protein was extracted by NP40 lysis buffer (Boster Biological Technology, Wuhan, China). Then the protein was precipitated with anti-flag antibody (MBL, Nagoya, Japan) or normal mouse IgG (Santa Cruz Biotechnology, Santa Cruz, CA, USA). The protein A/G PLUS-Agarose beads (Santa Cruz Biotechnology) were then added. The purified protein was subjected to western blot analysis using Clean-Blot IP Detection Reagent (Thermo Fisher Scientific) as the secondary antibody.

Immunofluorescence

Cells cultured on glass coverslips were fixed with 4% paraformaldehyde and incubated with the primary antibodies. The liver tissue sections were fixed with 4% paraformaldehyde, embedded in paraffin, and were incubated with the primary antibodies. The primary and secondary antibodies are listed in Table S3. At last, DAPI (Beyotime, Shanghai, China) was used to counterstain the nuclei, and the images were captured using an Olympus IX71 fluorescence microscope with a DP73 Microscope camera (Olympus).

Dataset analysis

The cDNA microarray data (GEO database: GSE28619) and RNA sequencing data (GEO database: GSE155907) were used for relevant analysis. R Studio software (Version 1.2.5033, RStudio, Boston, MA, USA) was used to convert the probes into gene names.

Statistical analysis

The data were presented as the means ± standard deviation (SD). The statistical significance of the difference was analyzed by Student's t test. Pearson correlation analysis was used to analyze the correlation between two variables. $p < 0.05$ was regarded as statistically significant. In this study, the statistical analyses were performed using GraphPad Prism 8 software (GraphPad Software, San Diego, CA, USA).

SUPPLEMENTAL INFORMATION

Supplemental information can be found online at https://doi.org/10.1016/j.omtn.2021.12.017.

ACKNOWLEDGMENTS

This study was supported by grants from the National Natural Science Foundation of China, China [grant number: 81873976, 31770837] and the Key Research and Development Program of Shandong Province, China [grant number: 2019GSF108148].

AUTHOR CONTRIBUTIONS

L.K.Z. and Y.N.X. conceived this study, generated hypotheses, and designed experiments. J.T., J.Z., M.K.W., Y.F.W., M.Z.D., and X.F.M. performed the experiments. J.T., B.K.S., and S.S.L. collected and analyzed the data. L.K.Z. and J.T. drafted the manuscript. Z.Z.Z., L.Z.C., W.W.J., Y.N.X., and K.L. revised the manuscript.

DECLARATION OF INTERESTS

All authors declare no conflicts of interest.

REFERENCES

1. Wei, M., Zhu, Z., Wu, J., Wang, Y., Geng, J., and Qin, Z.H. (2019). DRAM1 deficiency affects the organization and function of the Golgi apparatus. Cell. Signal. *63*, 109375.

2. Kerley-Hamilton, J.S., Pike, A.M., Hutchinson, J.A., Freemantle, S.J., and Spinella, M.J. (2007). The direct p53 target gene, FLJ11259/DRAM, is a member of a novel family of transmembrane proteins. Biochim. Biophys. Acta. *1769*, 209–219.

3. Crighton, D., Wilkinson, S., O'Prey, J., Syed, N., Smith, P., Harrison, P.R., Gasco, M., Garrone, O., Crook, T., and Ryan, K.M. (2006). DRAM, a p53-induced modulator of autophagy, is critical for apoptosis. Cell *126*, 121–134.

4. Liu, K., Lou, J., Wen, T., Yin, J., Xu, B., Ding, W., Wang, A., Liu, D., Zhang, C., Chen, D., et al. (2013). Depending on the stage of hepatosteatosis, p53 causes apoptosis primarily through either DRAM-induced autophagy or BAX. Liver Int. *33*, 1566–1574.

5. Tang, N., Zhao, H., Zhang, H., and Dong, Y. (2019). Effect of autophagy gene DRAM on proliferation, cell cycle, apoptosis, and autophagy of osteoblast in osteoporosis rats. J. Cell. Physiol. *234*, 5023–5032.
6. Memmert, S., Nogueira, A.V.B., Damanaki, A., Nokhbehsaim, M., Eick, S., Divnic-Resnik, T., Spahr, A., Rath-Deschner, B., Till, A., Götz, W., et al. (2018). Damage-regulated autophagy modulator 1 in oral inflammation and infection. Clin. Oral Investig. *22*, 2933–2941.
7. Avila, M.A., Dufour, J.F., Gerbes, A.L., Zoulim, F., Bataller, R., Burra, P., Cortez-Pinto, H., Gao, B., Gilmore, I., Mathurin, P., et al. (2020). Recent advances in alcohol-related liver disease (ALD): summary of a Gut round table meeting. Gut *69*, 764–780.
8. Thursz, M., Kamath, P.S., Mathurin, P., Szabo, G., and Shah, V.H. (2019). Alcohol-related liver disease: areas of consensus, unmet needs and opportunities for further study. J. Hepatol. *70*, 521–530.
9. Griswold, M.G., Fullman, N., Hawley, C., Arian, N., Zimsen, S.R.M., Tymeson, H.D., Venkateswaran, V., Tapp, A.D., Forouzanfar, M.H., and Salama, J.S. (2018). Alcohol use and burden for 195 countries and territories, 1990-2016: a systematic analysis for the Global Burden of Disease Study 2016. Lancet *392*, 1015–1035.
10. Kong, L.Z., Chandimali, N., Han, Y.H., Lee, D.H., Kim, J.S., Kim, S.U., Kim, T.D., Jeong, D.K., Sun, H.N., Lee, D.S., et al. (2019). Pathogenesis, early diagnosis, and therapeutic management of alcoholic liver disease. Int. J. Mol. Sci. *20*, 2712.
11. Amini, M., and Runyon, B.A. (2010). Alcoholic hepatitis 2010: a clinician's guide to diagnosis and therapy. World. J. Gastroenterol. *16*, 4905–4912.
12. Naveau, S., Chollet-Martin, S., Dharancy, S., Mathurin, P., Jouet, P., Piquet, M.A., Davion, T., Oberti, F., Broët, P., and Emilie, D. (2004). A double-blind randomized controlled trial of infliximab associated with prednisolone in acute alcoholic hepatitis. Hepatology *39*, 1390–1397.
13. Szabo, G. (2015). Gut-liver axis in alcoholic liver disease. Gastroenterology *148*, 30–36.
14. Verma, V.K., Li, H., Wang, R., Hirsova, P., Mushref, M., Liu, Y., Cao, S., Contreras, P.C., Malhi, H., Kamath, P.S., et al. (2016). Alcohol stimulates macrophage activation through caspase-dependent hepatocyte derived release of CD40L containing extracellular vesicles. J. Hepatol. *64*, 651–660.
15. Ge, X., Leung, T.M., Arriazu, E., Lu, Y., Urtasun, R., Christensen, B., Fiel, M.I., Mochida, S., Sørensen, E.S., and Nieto, N. (2014). Osteopontin binding to lipopolysaccharide lowers tumor necrosis factor-α and prevents early alcohol-induced liver injury in mice. Hepatology *59*, 1600–1616.
16. Dou, L., Shi, X., He, X., and Gao, Y. (2019). Macrophage phenotype and function in liver disorder. Front. Immunol. *10*, 3112.
17. Li, H.D., Chen, X., Xu, J.J., Du, X.S., Yang, Y., Li, J.J., Yang, X.J., Huang, H.M., Li, X.F., Wu, M.F., et al. (2020). DNMT3b-mediated methylation of ZSWIM3 enhances inflammation in alcohol-induced liver injury via regulating TRAF2-mediated NF-κB pathway. Clin. Sci. (Lond). *134*, 1935–1956.
18. Slevin, E., Baiocchi, L., Wu, N., Ekser, B., Sato, K., Lin, E., Ceci, L., Chen, L., Lorenzo, S.R., Xu, W., et al. (2020). Kupffer cells: inflammation pathways and cell-cell interactions in alcohol-associated liver disease. Am. J. Pathol. *190*, 2185–2193.
19. Kong, Q., Li, N., Cheng, H., Zhang, X., Cao, X., Qi, T., Dai, L., Zhang, Z., Chen, X., Li, C., et al. (2019). HSPA12A is a novel player in nonalcoholic steatohepatitis via promoting nuclear PKM2-mediated M1 macrophage polarization. Diabetes *68*, 361–376.
20. Elsharkasy, O.M., Nordin, J.Z., Hagey, D.W., de Jong, O.G., Schiffelers, R.M., Andaloussi, S.E., and Vader, P. (2020). Extracellular vesicles as drug delivery systems: Why and how? Adv. Drug Deliv. Rev. *159*, 332–343.
21. Mead, B., and Tomarev, S. (2020). Extracellular vesicle therapy for retinal diseases. Prog. Retin. Eye Res. *79*, 100849.
22. Wiklander, O.P.B., Brennan, M., Lötvall, J., Breakefield, X.O., and El Andaloussi, S. (2019). Advances in therapeutic applications of extracellular vesicles. Sci. Transl. Med. *11*, eaav8521.
23. Azparren-Angulo, M., Royo, F., Gonzalez, E., Liebana, M., Brotons, B., Berganza, J., Goñi-de-Cerio, F., Manicardi, N., Abad-Jordà, L., Gracia-Sancho, J., et al. (2021). Extracellular vesicles in hepatology: physiological role, involvement in pathogenesis, and therapeutic opportunities. Pharmacol. Ther. *218*, 107683.
24. Thietart, S., and Rautou, P.E. (2020). Extracellular vesicles as biomarkers in liver diseases: a clinician's point of view. J. Hepatol. *73*, 1507–1525.
25. Mandrekar, P., and Szabo, G. (2009). Signalling pathways in alcohol-induced liver inflammation. J. Hepatol. *50*, 1258–1266.
26. Seitz, H.K., Bataller, R., Cortez-Pinto, H., Gao, B., Gual, A., Lackner, C., Mathurin, P., Mueller, S., Szabo, G., and Tsukamoto, H. (2018). Alcoholic liver disease. Nat. Rev. Dis. Primers. *4*, 16.
27. Kreimer, S., Belov, A.M., Ghiran, I., Murthy, S.K., Frank, D.A., and Ivanov, A.R. (2015). Mass-spectrometry-based molecular characterization of extracellular vesicles: lipidomics and proteomics. J. Proteome. Res. *14*, 2367–2384.
28. Hou, P.P., Luo, L.J., Chen, H.Z., Chen, Q.T., Bian, X.L., Wu, S.F., Zhou, J.X., Zhao, W.X., Liu, J.M., Wang, X.M., et al. (2020). Ectosomal PKM2 promotes HCC by inducing macrophage differentiation and remodeling the tumor microenvironment. Mol. Cell. *78*, 1192–1206.e10.
29. Ni, P., Xu, H., Chen, C., Wang, J., Liu, X., Hu, Y., Fan, Q., Hou, Z., and Lu, Y. (2012). Serum starvation induces DRAM expression in liver cancer cells via histone modifications within its promoter locus. PLoS. One. *7*, e50502.
30. Yu, M., Jiang, Y., Feng, Q., Ouyang, Y., and Gan, J. (2014). DRAM1 protects neuroblastoma cells from oxygen-glucose deprivation/reperfusion-induced injury via autophagy. Int. J. Mol. Sci. *15*, 19253–19264.
31. Xu, J., Zang, Y., Liu, D., Yang, T., Wang, J., Wang, Y., Liu, X., and Chen, D. (2019). DRAM is involved in hypoxia/ischemia-induced autophagic apoptosis in hepatocytes. Aging Dis. *10*, 82–93.
32. Xu, L., Yu, Y., Sang, R., Li, J., Ge, B., and Zhang, X. (2018). Protective effects of taraxasterol against ethanol-induced liver injury by regulating CYP2E1/Nrf2/HO-1 and NF-κB signaling pathways in mice. Oxid. Med. Cell. Longev. *2018*, 8284107.
33. Sangineto, M., Grabherr, F., Adolph, T.E., Grander, C., Reider, S., Jaschke, N., Mayr, L., Schwärzler, J., Dallio, M., Moschen, A.R., et al. (2020). Dimethyl fumarate ameliorates hepatic inflammation in alcohol related liver disease. Liver Int. *40*, 1610–1619.
34. Ho, C.J., Lin, R.W., Zhu, W.H., Wen, T.K., Hu, C.J., Lee, Y.L., Hung, T.I., and Wang, C. (2019). Transcription-independent and -dependent p53-mediated apoptosis in response to genotoxic and non-genotoxic stress. Cell. Death Discov. *5*, 131.
35. Ahn, B.Y., Trinh, D.L., Zajchowski, L.D., Lee, B., Elwi, A.N., and Kim, S.W. (2010). Tid1 is a new regulator of p53 mitochondrial translocation and apoptosis in cancer. Oncogene *29*, 1155–1166.
36. Yu, G., Luo, H., Zhang, N., Wang, Y., Li, Y., Huang, H., Liu, Y., Hu, Y., Liu, H., Zhang, J., et al. (2019). Loss of p53 sensitizes cells to palmitic acid-induced apoptosis by reactive oxygen species accumulation. Int. J. Mol. Sci. *20*, 6268.
37. Yuan, H., Duan, S., Guan, T., Yuan, X., Lin, J., Hou, S., Lai, X., Huang, S., Du, X., and Chen, S. (2020). Vitexin protects against ethanol-induced liver injury through Sirt1/p53 signaling pathway. Eur. J. Pharmacol. *873*, 173007.
38. Yan, Z., Miao, X., Zhang, B., and Xie, J. (2018). p53 as a double-edged sword in the progression of non-alcoholic fatty liver disease. Life Sci. *215*, 64–72.
39. McGill, G., and Fisher, D.E. (1999). p53 and cancer therapy: a double-edged sword. J. Clin. Invest. *104*, 223–225.
40. Alquraishi, M., Puckett, D.L., Alani, D.S., Humidat, A.S., Frankel, V.D., Donohoe, D.R., Whelan, J., and Bettaieb, A. (2019). Pyruvate kinase M2: a simple molecule with complex functions. Free Radic. Biol. Med. *143*, 176–192.
41. Hsu, M.C., and Hung, W.C. (2018). Pyruvate kinase M2 fuels multiple aspects of cancer cells: from cellular metabolism, transcriptional regulation to extracellular signaling. Mol. Cancer *17*, 35.
42. Yang, L., Xie, M., Yang, M., Yu, Y., Zhu, S., Hou, W., Kang, R., Lotze, M.T., Billiar, T.R., Wang, H., et al. (2014). PKM2 regulates the Warburg effect and promotes HMGB1 release in sepsis. Nat. Commun. *5*, 4436.
43. Palsson-McDermott, E.M., Curtis, A.M., Goel, G., Lauterbach, M.A., Sheedy, F.J., Gleeson, L.E., van den Bosch, M.W., Quinn, S.R., Domingo-Fernandez, R., Johnston, D.G., et al. (2015). Pyruvate kinase M2 regulates Hif-1α activity and IL-1β induction and is a critical determinant of the warburg effect in LPS-activated macrophages. Cell. Metab. *21*, 65–80.
44. Meoli, L., Gupta, N.K., Saeidi, N., Panciotti, C.A., Biddinger, S.B., Corey, K.E., and Stylopoulos, N. (2018). Nonalcoholic fatty liver disease and gastric bypass surgery regulate serum and hepatic levels of pyruvate kinase isoenzyme M2. Am. J. Physiol. Endocrinol. Metab. *315*, E613–E621.
45. Amin, S., Yang, P., and Li, Z. (2019). Pyruvate kinase M2: a multifarious enzyme in non-canonical localization to promote cancer progression. Biochim. Biophys. Acta. Rev. Cancer *1871*, 331–341.